Shear-Strain Measurement in Solid-Propellant Rocket Motors

G. M. DICKEN* AND J. H. THACHER†
Hercules Powder Company, Cumberland, Md.

To assess structural integrity of rocket motors, it is essential to know grain stresses and strains. Unfortunately, techniques for reliably measuring stresses and strains are, for the most part, undeveloped. This paper describes the development of an experimental method for measuring shear strain in propellant at the case-bond. A new, low-modulus, d.c., semiconductor shear-strain transducer (gage) is described; it has been used to measure case-bond shear strains in inert loaded rocket motors subjected to axial and transverse accelerations up to nearly 50 g. Results are shown to be in good agreement with theoretical analysis of a relatively simple grain design. Proposed use of the transducer in live-propellant rocket motors is outlined.

Nomenclature

a = inner radius of grain, in.
b = outer radius of grain, in.
$D(t)$ = tensile creep compliance $(\text{psi})^{-1}$
E = tensile modulus of elasticity, psi
$g(t)$ = time-dependent acceleration (number of g's)
$g_k(t)$ = ramp component of acceleration (number of g's)
$H(t)$ = Heaviside step function; equals unity when $t > 0$ and zero when $t < 0$
i, k = summation indices
$J(t)$ = shear creep compliance $(\text{psi})^{-1}$
Q = geometric factor defined by Eq. (10)
r = radius, in.
s = Laplace transform parameter $(\text{sec})^{-1}$
T = temperature, °F
t = time, sec
w = axial displacement, in.
γ = shearing strain, rad
λ = dummy variable of integration, sec
ν = Poisson's ratio
ρ = weight density of propellant, lb-force/in.^{3}
τ = shearing stress, psi
θ = angle measured from the vertical, rad
$(\bar{\ })$ = Laplace transform; e.g.,

$$\bar{w}(s) = \int_0^\infty w(t)\, e^{-st}\, dt$$

Introduction

CRITICAL propellant and case-bond loading conditions in solid-propellant rockets are considered to be the conditions listed in Table 1. To evaluate structural margins of safety, existing stresses and strains and the ultimate properties of the propellant and case-bond must be known. Generally, however, complex grain configurations, involved time- and temperature-dependent propellant properties, and large deformations make it impossible to find exact theoretical solutions for stresses and strains. For this reason, experimental stress and strain measurements, such as those made with the use of the shear-strain transducer described in this paper, take on increased importance.

This paper begins with a survey of existing and/or proposed stress-strain measuring devices. The new low-modulus, d.c. semiconductor transducer and the evaluation test procedure are then described. The test procedures used to characterize the inert propellant used in this work are given. The grain structural analysis is then presented and utilized to evaluate experimental results. Finally, the proposed use of the transducer in live-propellant rocket motors is outlined.

Presented as Preprint 64-506 at the 1st AIAA Annual Meeting, Washington, D. C., June 29–July 2, 1964; revision received November 4, 1964.

* Project Engineer, Allegany Ballistic Laboratory.
† Senior Research Engineer, Allegany Ballistic Laboratory.

Survey of Methods to Measure Stresses and Strains in Propellant

Simple Wire Strain-Gage Method

One-mil-diam, high-elongation (KARMA and ADVANCE)‡ strain-gage wires have been unidirectionally embedded in dummy propellant tensile specimens. The electrical resistance change caused by strain in the embedded wire (bonded to the propellant) was believed to be a measure of propellant strain. Unfortunately, the considerable reinforcement effect of the wire makes such high-modulus materials unsuitable for measuring propellant strain.

Propellant Port Displacement Method

Although not conveniently adaptable to measuring strains of a firing rocket motor grain, the following devices have been used with varying degrees of success to determine displacement of the propellant port surface in pressurized simulated grains and in unfired motors subjected to axial accelerations: 1) dial gages, 2) linear potentiometers, 3) spring clip gages using magnetometer detection, and 4) steel pellet/x-ray movies.

Flux Gage Magnetometer Method

It has been suggested that the embedded pellet and x-ray techniques used in highly successful laboratory tests might be extended to a flight application wherein small lightweight magnetometers with three sensing heads could locate by triangulation the positions of lightweight magnetic embedded pellets. This system, which does not require strain-perturbing leads through the propellant, might also be used to determine the burning surface of propellant. Allegany Ballistics Laboratory (ABL) work has shown that the technique is 1% accurate in determining strains of the order of 15%. Prob-

Table 1 Critical conditions in solid propellant rockets

Loading	Potential problem area
Pressurization	Maximum hoop strain at port radius or star root
Thermal	Case-bond and/or grain failure during temperature cycling; grain collapse and/or star root strain for positive ΔT
Acceleration: axial, transverse, and angular	Case-bond shear and normal strength in cylinder and dome areas; excessive grain deformation

‡ Trade-mark of the Driver Harris Company, Harrison, N. J.

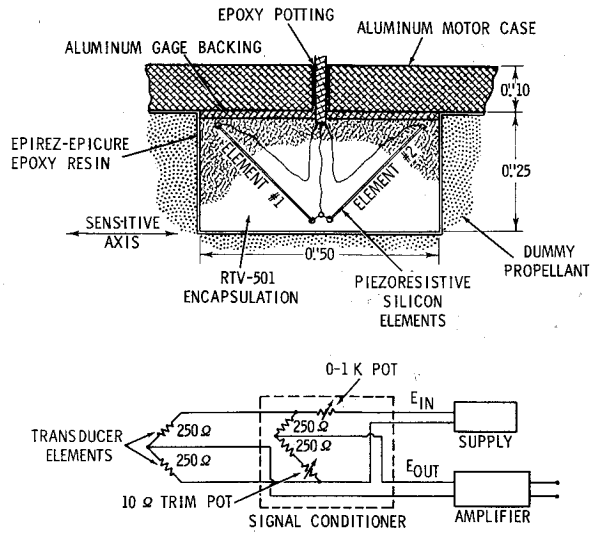

Fig. 1 Case-bond shear-strain gage.

lems anticipated with this system are interacting magnetic fields and a hardware weight penalty.

Durelli[1] has reviewed additional methods employing the following measuring devices, the first for use on propellant surface, and the other five for use within the propellant grains: 1) surface strain gage on propellant-like material, 2) embedded strain capsule, 3) helical or coil strain gages, 4) pneumatic and hydraulic gages, 5) capacitance gages, and 6) conductive rubber gages. Problems of interaction between propellant and measuring device are anticipated for all of these methods. Lead wires, resulting in further perturbation of strains, are normally required in all these methods. Mechanical reinforcement by the gage disturbing the local strain field is a problem in devices 2–5. Calibration, sensitivity, and stability may be a problem with conductive rubber gages. The measurement of surface strains by strain gages presents a mechanical reinforcement problem, and other methods for surface strain measurement such as use of optical boroscope, replicate techniques, photoelastic coating or Moiré fringe are not adaptable to measurement of strains during static firing or flight.

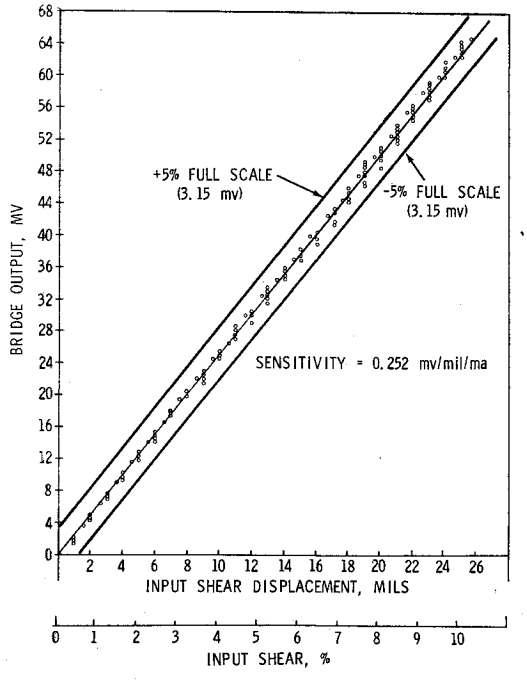

Fig. 2 Repeatability test for increasing shear.

One important area that has been neglected is propellant shear measurements; no shear measuring devices are now commercially available. To fill this need, a project was started to develop the shear-strain measuring device described in the next section.

Description of Shear-Strain Transducer

The transducer used in the work is a new low-modulus, d.c. semiconductor, shear-strain gage, which was developed for ABL by Gulton Industries, Inc., Metuchen, N. J.[2] The gage consists essentially of two piezoresistive silicon elements, each mounted at a 45° angle with respect to the sensitive axis and perpendicular to each other (Fig. 1). The elements are electrically connected to form a Wheatstone bridge with two active arms and two arms in an external signal conditioning module. Under the effects of normal strain input (tension or compression resulting from thermal shrinkage or pressurization), the elements suffer the same resistance changes, and the bridge remains in balance. For shear-strain input in the sensitive direction, one element contracts while the other element expands. This action results in a bridge unbalance, the magnitude of which is proportional to the shear-strain input; signal polarity gives the direction of the input strain. The gage output is fed into a signal conditioner and amplifier.

Encapsulation of the sensitive elements in a rubbery material results in more nearly matched mechanical impedances between propellant and gage than is possible with an unencapsulated gage. The rubbery encapsulation also imposes only small strain upon the elements, thereby avoiding problems of hysteresis, creep, and loss of linearity. Under these conditions the strain range input to the gage is also extended far beyond that which could be obtained with the relatively stiff and sensitive elements used without encapsulation.

The gage also has a potential for measuring normal strain input simultaneously with shear by measuring the output from each element separately during a shear-strain measurement. Normal strain measurements have not been made at the time of this writing; however, tests are planned. In the present gages, temperature compensation is provided by selecting carefully matched elements. Gage specifications are listed in Table 2. The original objective was to develop a gage that would measure 0–1% shear strain; however, the developed gage was found to have an effective range of 0–10% shear strain. Repeatability is demonstrated in Fig. 2.

Table 2 Specifications for the d. c. flexible shear gage

Gage characteristics	Specifications
Sensitive elements	Piezoresistive silicon
Operation	2-active-arm Wheatstone bridge
Encapsulation	RTV-501 silicone rubber
Measurement	One-dimensional shear between case and propellant
Basic gage size	$\frac{1}{2}$ in. in shear sensitive direction × $\frac{1}{4}$ in. × $\frac{1}{4}$ in.
Readout wire	2 or 3 conductor-sheathed cable, 3 ft long (minimum) × 0.0625-in. o.d. (maximum)
Maximum element power dissipation	0.1 w
Temperature sensitivity	±5% full scale over range
Temperature range	Operating: 60°F to 80°F; motor cure environment: maximum 4 days at 180°F
Shear range and readout	0–5 v d.c., full scale, for 0 to 1% shear-strain input; good to 10% shear-strain input (sensitivity of gages supplied to ABL vary from 0.15 to 0.29 mv/mil/ma)
Linearity, hysteresis, and repeatability	±5% full scale

Bench scale calibration was accomplished by deformation of the gage encapsulation using guide plates bonded to opposite faces of the gage and a precision micrometer head. Gage sensitivity can be varied by changing the modulus of elasticity of the room temperature vulcanizing (RTV) silicone rubber encapsulation material through formulation modifications. More important is the fact that the modulus of the RTV can be made to approximate that of the solid propellant in which the gage will be used.

The problem of the gage itself modifying the strain distribution has been minimized by proper selection of the encapsulating material. In addition, the good agreement between theoretical and experimental data indicates that the gage does not significantly change strain patterns. Photoelastic studies have been made for gages composed of similar piezoresistive elements encapsulated in silicone rubber and used in propellant-like materials. These studies demonstrate that severe strain gradients caused by the presence of the gage are localized to a region within 0.05 in. of the gage.[3]

The strains reported in this paper are averaged over the thickness of the gage. Definitive tests using varying dimensions of encapsulation are planned to determine the region of gage reinforcement. If a sufficiently large region is used, the gage will give average readings within a given tolerance of unreinforced propellant strains.

Description of Centrifuge Tests

Initial tests were made with the gages installed in the inert ("dummy") propellant to measure axial and transverse strains in the motor midsection during a centrifuge test (Fig. 3). The test motor was a simple cylindrical design weighing approximately 35 lb loaded. The motor was attached 26 ft from the center of rotation of the centrifuge arm. Present capability of the diesel-powered centrifuge in testing small rocket motors is approximately 80 rpm, corresponding to 57 g. The centrifuge is equipped with ten slip rings for data acquisition, but additional channels may be obtained by using selective sampling procedures.

The first test motor was accelerated to 43 g axially, then rotated and accelerated to 43 g transversely. A typical acceleration vs time curve for the ABL centrifuge is shown in Fig. 4. In each of these tests, one gage measured shear strain significantly higher than the predicted (theoretical) strain. A region of soft, partially cured material was observed in the area that would affect these two gages. In contrast, the other two gages measured strains close to predicted strains.

In another test, a similar motor was equipped with six shear-strain gages to determine propellant case-bond "end-effects" under axial acceleration. Gages were installed inside the motor case, two at each end and two at the midsection, aligned for axial sensitivity. The inert grain was cast

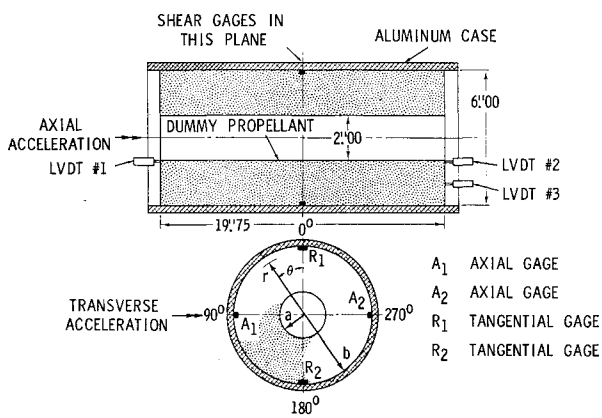

Fig. 3 Motor with case-bond shear-gages installed.

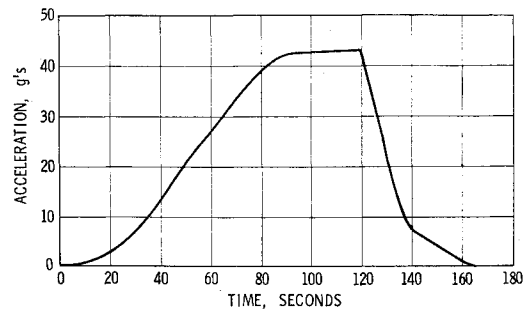

Fig. 4 Typical acceleration curve for ABL centrifuge.

so that it would extend $\frac{1}{4}$ in. beyond the gages at each end. This motor was accelerated to 42 g axially. Maximum shear strains measured indicate that no serious stress concentrations were present at the gages at the end of the motor.

The dummy propellant is a copolymer of butadiene and acrylic acid crosslinked with a diepoxide resin and filled with spherical 10-μ aluminum; it is a homogeneous, isotropic, linear viscoelastic material. Homogeneity was verified by testing many samples; isotropy was ascertained by casting hollow cylinders and comparing samples cut in the hoop and axial directions.[4] The range of stresses over which linear viscoelasticity was applicable was determined by measuring tensile creep compliance at a series of increasing stress levels. The minimum stress at which the creep compliance no longer agreed with the value at lower stresses was defined as the limit of linear viscoelasticity. This limit (10 psi) was above the stress level (5 psi) of the centrifuge test.

The shear creep compliance was determined from the measured tensile creep compliance $D(t)$ using the relation

$$J(t) = 2(1 + \nu)\, D(t)$$

where it is assumed that Poisson's ratio is independent of time. The value of Poisson's ratio ($\nu = 0.4993$) determined from bulk modulus measurements and the tensile creep compliance shows that the material is nearly incompressible.

Discussion of Results

Results of two axial acceleration tests are shown in Fig. 5. The gages measured strains that were in close agreement with strains predicted using the theory presented in the Appendix. The general shape of the predicted time-dependent response is followed closely.

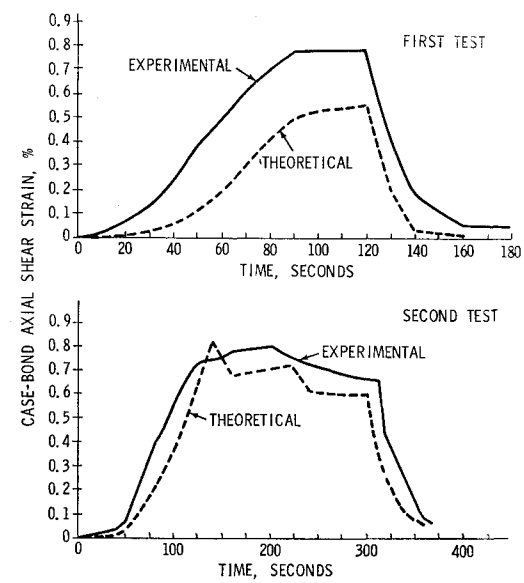

Fig. 5 Axial acceleration test results.

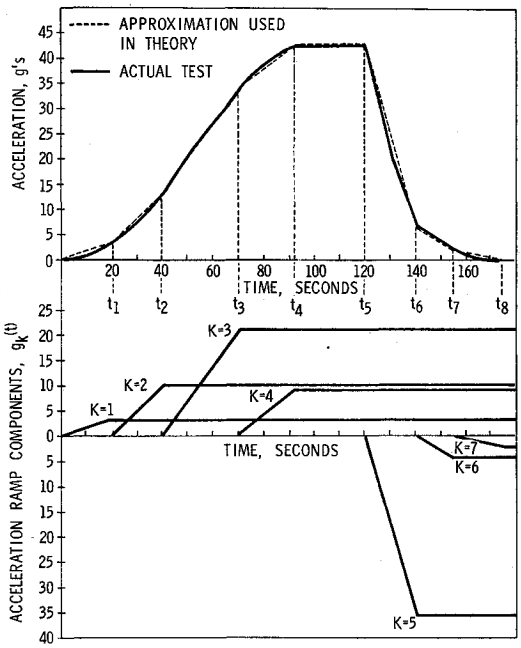

Fig. 6 Decomposition of centrifuge loading to approximate ramp components.

In the recent end-effects test, case-bond shear strains measured by gages located $\frac{1}{4}$ in. from the end of the motor show that no stress concentration effects are present at this location. As predicted by theory, the stress decreases to its average value a very short distance from the end. Further, the measured shear strain is averaged over the length of the gage. This does not eliminate the possibility of stress concentration effects in a very small area adjacent to the case-bond at the very end of the grain.

In the transverse shear test, the predicted case-bond shear strain was 0.37%; the gage measured 0.39% in a motor accelerated to 43 g. These calculations are preliminary, but the agreement between theory and experiment is encouraging. Further work will consider a compressible viscoelastic propellant bonded to an elastic case. The solution by Gillis,[5] based on the work of Muskhelishvili[6] and Lianis,[7] will be applied to this test motor.

Application to Live-Propellant Grains

No major obstacles are foreseen in the use of this gage in a full-scale, live-propellant rocket motor. Such gage applications, however, will differ in several respects from applications to inert test material, but it is expected that the gage can be modified to meet all these requirements. For instance, the gage may require modification to measure strains up to 30%. Additional requirements of increased chemical and thermal resistance and safety should give no difficulty. The RTV silicone rubber encapsulation should provide adequate protection against the low molecular weight esters present in the propellant manufacturing process.

Shear-strain transducers exposed for 19 hr to 184°F, a higher temperature than any employed in curing commonly used propellants, reproduced readings taken before exposure. In another test, the gage was exposed to propellant cure temperature (120°F) for four days with no change in repeatability. Consequently, the gage is not expected to be affected by the propellant curing process.

As to the safety requirements, the gage has been so designed that it will not accidentally ignite the propellant. The current, voltage, and power levels are well below the levels required to ignite propellant. Maximum current, voltage, and power levels within the gage are 10 ma, 6 v, and 0.1 w, respectively; strain gages placed in composite-modified, double-base propellants with aluminum filler have been subjected to 83 ma, 10 v, and 8 w without igniting the propellant.

Methods of placing the gage within the propellant grain and getting the signal out are necessary. Since accelerometers have been successfully installed within a propellant grain without lead wire problems,[8] it is concluded that techniques are available for installing shear-strain gages within a propellant grain. Lead wire and gage reinforcement effects remain to be defined with additional testing.

Testing of this shear-strain gage is considered sufficiently successful to use this gage or an improved version in tests involving live-propellant rocket motors. With increased confidence in this gage and/or other "in-grain" instrumentation, stress analyses and structural margins of safety will be made for conditions not presently covered by theory.

Conclusions

A semiconductor transducer has been developed which is capable of measuring shear strains in low-modulus propellant-like materials. It has been evaluated under axial and transverse accelerations up to nearly 50 g. There was good agreement between theoretical and experimental data. Although the application of the transducer to live propellant will differ in several respects from its application to inert grains, it is expected that the gage can be modified to meet all requirements.

Appendix

Infinite Length Cylinder, Axial Acceleration

The linear viscoelastic theory used to interpret centrifuge test results is presented in this section. The hollow case-bonded cylindrical grain is shown in Fig. 3. The length/diameter ratio is sufficiently large that only axial shear stresses and strains need to be considered.§

A force balance in the axial or z direction on a differential element gives the equation of motion

$$\partial(r\tau)/\partial r = \rho g r \tag{A1}$$

This equation states that acceleration body forces are balanced by propellant shearing stresses.

The strain displacement equation (in the absence of radial displacements),

$$\gamma = \partial w/\partial r \tag{A2}$$

relates the angle of distortion of a differential element to the axial displacement.

The shear stress-strain relation for a linear viscoelastic material is[9]

$$\gamma = \int_{-\infty}^{t} J(t-\lambda)\left(\frac{d\tau}{d\lambda}\right) d\lambda \tag{A3}$$

The boundary conditions $w(b) = 0$ and $\tau(a) = 0$ describe a rigid case and a stress-free port.

The field Eqs. (A1–A3) and the boundary conditions completely define the problem. Since the Laplace transform method of solution is used, the required transforms are applied directly to the equation of motion and the strain displacement relation:

$$\partial(r\bar{\tau})/\partial r = \rho \bar{g} r \tag{A4}$$

$$\bar{\gamma} = \partial \bar{w}/\partial r \tag{A5}$$

§ Solutions by the method of variation of potential energy[10] and by a finite difference method using Southwell stress functions[11] show that end-effects are small for this motor. There is, however, always a local stress concentration at the case-bond at the ends of the motor. The theory of singularities[12] predicts a large stress gradient in the neighborhood of this stress concentration.

The stress-strain relation is a convolution-type integral; for zero initial conditions and a sample undisturbed prior to zero time,¶ its Laplace transform is

$$\bar{\gamma} = s\bar{J}(s)\bar{\tau} \tag{A6}$$

and the transformed boundary conditions are $\bar{w}(b) = 0$ and $\bar{\tau}(a) = 0$.

Substitution of Eq. (A6) into Eq. (A4) and subsequent use of Eq. (A5) gives the Laplace transformed equation of motion

$$\frac{\partial}{\partial r}\left[\frac{r\,\partial\bar{w}}{s\bar{J}(s)\partial r}\right] = \rho\bar{g}r \tag{A7}$$

whose solution is

$$\bar{w} = \tfrac{1}{4}\rho\bar{g}s\,\bar{J}(s)r^2 + C_1\ln r + C_2 \tag{A8}$$

Here, C_1 and C_2 are arbitrary functions of the Laplace transform parameters. They are evaluated from the transformed boundary conditions, and it follows that

$$\bar{w} = Q\bar{g}s\bar{J}(s) \tag{A9}$$

where Q is a time independent factor

$$Q = \rho/2\{[(r^2 - b^2)/2] - a^2\ln(r/b)\} \tag{A10}$$

The solution for the axial displacement is obtained from the transformed displacement by application of the inverse Laplace transform. To accomplish this inversion, it is necessary to specify the acceleration loading program and the shear creep compliance. The acceleration loading program was split into a series of ramps as shown in Fig. 6. A single ramp beginning at t_k and reaching its maximum value at t_{k+1} is specified by

$$g_k(t) = \frac{(g_{k+1} - g_k)}{(t_{k+1} - t_k)}\,[(t - t_k)H(t - t_k) - (t - t_{k+1})H(t - t_{k+1})] \tag{A11}$$

Application of the Laplace transform yields

$$\bar{g}_k(s) = \frac{(g_{k+1} - g_k)}{s^2(t_{k+1} - t_k)}\,[\exp(-t_k s) - \exp(-t_{k+1}s)] \tag{A12}$$

Using a collocation data-fitting process, the creep compliance is expressed as a series

$$J(t) = J_0 + \sum_{i=1}^{N} J_i\left[1 - \exp\left(-\frac{t}{\tau_i}\right)\right] \tag{A13}$$

whose Laplace transform is

$$\bar{J}(s) = \frac{J_0}{s} + \sum_{i=1}^{N}\frac{J_i}{\tau_i s(s + 1/\tau_i)} \tag{A14}$$

For unloading, the creep function is replaced by the recovery function.

Substituting Eqs. (A12) and (A14) into Eq. (A9) and applying an inverse Laplace transform gives the axial displacement in response to a single generalized ramp acceleration loading:

$$w_k(g_k, t_k) = Q\frac{g_{k+1} - g_k}{t_{k+1} - t_k}\left[\left((t - t_k)\left(J_0 + \sum_{i=1}^{N} J_i\right) - \sum_{i=1}^{N} J_i\tau_i\left\{1 - \exp\left[-\frac{t - t_k}{\tau_i}\right]\right\}\right)H(t - t_k) - \left((t - t_{k+1})(J_0 + \sum_{i=1}^{N} J_i) - \sum_{i=1}^{N} J_i\tau_i\left\{1 - \exp\left[-\left(\frac{t - t_{k+1}2}{\tau_i}\right)\right]\right\}\right)H(t - t_{k+1})\right] \tag{A15}$$

¶ This assumption is not strictly true for materials that do not return to original dimensions after loads are removed and for materials with residual stresses. In effect, each time a material is loaded or unloaded (as when a grain is centrifuged), a new material results. Dimension recovery of the material used in these tests is nearly complete, so that the use of such an assumption to render the problem tractable is not considered a serious limitation.

Superposition of responses to all the component ramp functions with appropriate time shifts gives the total axial displacement

$$W = \sum_{k=1}^{M} w_k(g_k, t_k) \tag{A16}$$

with w_k defined by Eq. (A15).

Strain is obtained by differentiation: $\gamma = \partial W/\partial r$, and, in particular, at the case bond

$$\gamma_{\text{case bond}} = \partial W/\partial r|_{r=b} \tag{A17}$$

Equations (A14) and (A15) were programed on an IBM 7074 computer program developed by Hercules Powder Company (HPC)/Bacchus.

Transverse Acceleration Tests

To evaluate experimental measurements of shear strain under lateral inertial loadings, the following simplified theory was used. An infinitely long hollow cylindrical propellant grain was bonded to a rigid case. The propellant was assumed to be homogeneous, isotropic, elastic, and incompressible. Small-deformation theory was used. With these assumptions, the field equations of elasticity have been solved using the Airy stress function method.[13] The resulting shear strain at the case-bond is

$$\gamma_r\theta\Big|_{r=b} = \frac{-3g\rho b\,\cos\theta[(b/a)^4 - 1]}{2E(b/a)^2\,[(b/a)^4 + 1]} \tag{A18}$$

References

[1] Durelli, A. J., "Survey of strain measuring methods," Aerojet-General Corp. Rept. 0411-10F, U. S. Air Force Contract AF33(600)-40315, Appendix B (March 1962).

[2] Schwartz, D. S., "Development of unidirectional d.c. axial and radial flexible propellant shear strain transducers," Gulton Industries, Inc., Final Report to Hercules Powder Co., Purchase Order ABL-73197 (November 1963).

[3] Schwartz, D. S., "Three-dimensional propellant strain measuring transducer," Gulton Industries, Inc., Final Report to Hercules Powder Co., Purchase Order 0243-04325 (April 1963).

[4] Sharma, M. G. and Lim, C. K., "Mechanical properties of solid propellants for combined states of stress at various temperatures," Pennsylvania State Univ., Annual Report to Hercules Powder Co., Contract NOrd 16640, Subcontract 70 (September 1963).

[5] Gillis, G. F., "Elastic stresses and displacements induced in solid propellant rocket motors by transverse gravity forces," Rohm and Haas Co., Rept. P-62-13 (June 1962).

[6] Muskhelishvili, N. I., *Some Basic Problems of the Mathematical Theory of Elasticity* (P. Noordhoff, Ltd., Gronigen, Holland, 1953), 3rd ed.

[7] Lianis, G., "Stresses and strains in solid propellant during storage," ARS Paper 1592-61 (1961).

[8] Perdue, D. G. and Nay, M. B., "Embedment of internal instrumentation in propellant grains," Hercules Powder Co. Rept. MPO-270-4 (August 1963).

[9] Lee, E. H., "Viscoelastic stress analysis," *Structural Mechanics*, edited by J. N. Goodier and N. J. Hoff (Pergamon Press, New York, 1960), p. 462.

[10] Knauss, W. G., "Displacements in an axially accelerated solid propellant grain," Solid Propellant Information Agency, SPIA/PP14u, Vol. 1, pp. 175–194 (October 1961).

[11] Parr, C. H., "Deformations and stresses in axially aceclerated case-bonded solid propellant grains of finite length," Rohm and Haas Co., Rept. P-62-27 (April 1963).

[12] Zak, A. J., "Stress singularities in bodies of revolution," California Institute of Technology, GALCIT SM 62-29 (July 1962).

[13] Hoekel, T., "Structural analysis of the Long Range Typhon propellant configuration," Emerson Electric Manufacturing Co., Rept. 1505 to Hercules Powder Company, Purchase Order ABL 57422-E, Alteration 3, pp. B. O. 1–B. O. 6 (March 1963).